4684–4695 *Nucleic Acids Research, 2009, Vol. 37, No. 14* *Published online 8 June 2009*
doi:10.1093/nar/gkp473

The incorporation of the novel histone variant H2AL2 confers unusual structural and functional properties of the nucleosome

Sajad Hussain Syed[1], Mathieu Boulard[1,2], Manu Shubhdarshan Shukla[1], Thierry Gautier[1], Andrew Travers[3], Jan Bednar[4,5], Cendrine Faivre-Moskalenko[6], Stefan Dimitrov[1,*] and Dimitar Angelov[2,*]

[1]Université Joseph Fourier – Grenoble 1, INSERM Institut Albert Bonniot, U823, Site Santé-BP 170, 38042 Grenoble Cedex 9, [2]Université de Lyon, Laboratoire de Biologie Moléculaire de la Cellule, CNRS-UMR 5239/ INRA 1237/IFR128 Biosciences, Ecole Normale Supérieure de Lyon, 46 Allée d'Italie, 69364 Lyon cedex 07, France, [3]MRC Laboratory of Molecular Biology, Hills Road, Cambridge CB2 2QH, UK, [4]CNRS/UJF, Laboratoire de Spectrométrie Physique, UMR 5588, BP87, 140 Av. de la Physique, 38402 St. Martin d'Hères Cedex, France, [5]Charles University in Prague, Institute of Cellular Biology and Pathology, First Faculty of Medicine and Department of Cell Biology, Institute of Physiology, Academy of Sciences of the Czech Republic, Albertov 4, 128 01 Prague 2, Czech Republic and [6]Université de Lyon, Laboratoire de Physique, CNRS UMR 5672, Ecole Normale Supérieure de Lyon, 46 Allée d'Italie, 69364 Lyon cedex 07, France

Received January 9, 2009; Revised May 7, 2009; Accepted May 18, 2009

ABSTRACT

In this work we have studied the properties of the novel mouse histone variant H2AL2. H2AL2 was used to reconstitute nucleosomes and the structural and functional properties of these particles were studied by a combination of biochemical approaches, atomic force microscopy (AFM) and electron cryo-microscopy. DNase I and hydroxyl radical footprinting as well as micrococcal and exonuclease III digestion demonstrated an altered structure of the H2AL2 nucleosomes all over the nucleosomal DNA length. Restriction nuclease accessibility experiments revealed that the interactions of the H2AL2 histone octamer with the ends of the nucleosomal DNA are highly perturbed. AFM imaging showed that the H2AL2 histone octamer was complexed with only ~130 bp of DNA. H2AL2 reconstituted trinucleosomes exhibited a type of a 'beads on a string' structure, which was quite different from the equilateral triangle 3D organization of conventional H2A trinucleosomes. The presence of H2AL2 affected both the RSC and SWI/SNF remodeling and mobilization of the variant particles. These unusual properties of the H2AL2 nucleosomes suggest a specific role of H2AL2 during mouse spermiogenesis.

INTRODUCTION

Chromatin exhibits a repeating structure. The basic repeating unit of chromatin, the nucleosome, is formed upon wrapping of two superhelical turns of DNA around an octamer of core histones (two of each H2A, H2B, H3 and H4). The structures of the histone octamer and the nucleosome core particle were solved by X-ray crystallography (1–3). The histones within both the nucleosome and the histone octamer are constituted of structured histone fold domains and unstructured N-termini (2,3). The individual nucleosomes are connected by linker DNA and form the chromatin filament in this way. A fifth histone, termed linker histone, is associated with the linker DNA and it assists the folding of the chromatin filament into the 30 nm chromatin fiber (4–8).

The nucleosome is a repressive structure. It interferes with the cellular processes, which need access to naked DNA. The cell uses three main strategies to overcome the nucleosome barrier, namely posttranslational histone modifications, chromatin remodeling by ATP-consuming chromatin-remodeling machines and histone variants.

The N-termini of the histones play an essential role in the organization of both the chromatin fiber (9,10) and the mitotic chromosomes (11,12). The histone posttranslational modifications are essentially located at the nonstructured N-termini of the histones. They can affect both the compaction of the chromatin fiber and the ability of remodeling machines to mobilize nucleosomes [for a

*To whom correspondence should be addressed. Tel: +33 4 72 72 88 98; Fax: +33 4 72 72 80 80; Email: dimitar.anguelov@ens-lyon.fr
Correspondence may also be addressed to Stefan Dimitrov. +33 4 76 54 94 73; +33 4 76 54 95 95; Email: stefan.dimitrov@ujf-grenoble.fr

recent review see (13)]. A typical example for such role of the histone modifications is the acetylation of the core histones (14,15) and in particular the acetylation of histone H4 at K16 (16). Histone modifications serve also as marks. These marks are recognized by specific protein factors, which in turn have important functional consequences (13,17).

The chromatin remodelers are high molecular multiprotein complexes, which are able, at the expenses of ATP hydrolysis, to mobilize the nucleosomes. The chromatin remodelers are required for several vital cellular processes, including transcription, replication and DNA repair. They are grouped in four distinct families: SWI2/SNF2, ISWI, CHD and INO80 (18). SWI/SNF and RSC (both belonging to the SWI2/SNF2 family), in addition to their capacity to mobilize the nucleosomes, are also able to alter significantly the structure of the nucleosomal particle and even to evict the histone octamers (19,20).

Histone variants are non-allelic isoforms of conventional histones (21). They show a variable degree of homology with their conventional counterparts [for a recent review see (22)]. All core histones, with the exception of H4, have histone variants. The H2A histone variants form the largest family of histone variants, including macroH2A, H2A.Z, H2A.X, H2A.Bbd, etc. Recently, a novel histone mouse variant H2AL2, belonging to the H2A family, was described (23). Polymerase chain reaction (PCR) experiments showed that H2AL2 is expressed in different tissues, but its expression was found to be remarkably strong during spermatogenesis (23).

The incorporation of some of the histone variants within the nucleosomes resulted in alterations of its structure, which in turn, affected its functional properties (24–27). The most striking example is H2A.Bbd. H2A.Bbd nucleosomes exhibited strong perturbations all over the nucleosomal DNA, these perturbations being stronger around the dyad axis (25,28,29). H2A.Bbd histone octamer was able to wrap only ~130 bp of DNA and H2A.Bbd nucleosomes exhibited very low stability both *in vitro* (25,26,28,29) and *in vivo* (30). In addition, the remodeling complexes SWI/SNF and ACF were unable to both remodel and mobilize the H2A.Bbd nucleosomes. Polymerase II activated transcription was more efficient from H2A.Bbd nucleosomal arrays than from conventional H2A templates (26,28). The unusual docking domain of H2A.Bbd was important in determining these particular properties of the H2A.Bbd chromatin (26,28).

In this work, we have focused on the recently identified histone H2AL2. We confirmed the reported data that H2AL2 is expressed exclusively in testis and we have studied the structural and functional properties of the H2AL2-reconstituted nucleosomes. We show that the incorporation of this sperm-specific histone variant within the nucleosomes altered its structural properties dramatically. These structural perturbations affected both the remodeling and the relocation of the H2AL2 nucleosomes induced by either SWI/SNF or RSC chromatin remodelers.

MATERIALS AND METHODS

H2AL2 cloning and preparation of DNA fragments

The H2AL2-coding sequence was amplified by PCR by using the EST IMAGE clone 6774311 cDNA and the primers 5′–TTTTCCTGGCCATATGGCCAGGAAAA GGCAAAGG-3′ (forward) and 5′–TGAGGATCCTCA GTTGTCATCAGGTTCTGGT–3′ (reverse). The PCR product was cloned between the restriction sites Nde I and BamH I in a pET3a vector (Novagen).

The 255-bp DNA fragments, containing the 601 nucleosome positioning sequence at the middle, were obtained by PCR amplification from plasmid pGem-3Z-601 (kindly provided by J. Widom and B. Bartholomew). The fragment was labeled either by incorporating the [α-^{32}P]CTP and [α-^{32}P]TTP to the PCR reaction for micrococcal digestion experiments or by 5′ labeling one of the primers for exonuclease and hydroxyl radical footprinting experiments.

For 'One Pot Restriction enzyme Assay' a set of eight pGEM-3Z-601.2 mutants was utilized, each containing Hae III site at a different superhelical location, as described before (31). Similarly, the 5′ labeled 147-bp core particle sequences were obtained by PCR amplification. The same fragments were used for DNase I footprinting experiments.

The 200-bp DNA fragment, containing the 601 nucleosome positioning sequence at the end of the fragment was obtained by cutting the 255 bp 601 with Not I. It was labeled with Klenow enzyme with [α-^{32}P]CTP in the presence of 50 μM dGTP. All the labeled probes were gel purified by 5% native acrylamide gel. DNA containing three repeats of the 601 sequence was constructed by using standard methods. The 33x 200–601 DNA was produced as reported (4) and nucleosomal array reconstituted by salt dialysis.

Protein purification and nucleosome reconstitution

Xenopus laevis histone proteins were produced in bacteria and purified as described (32). Recombinant H2AL2 protein was also purified like other histone proteins by usual process of IPTG induction, inclusion body solubilization and ion exchange purification. RSC and SWI/SNF were purified from yeast cells by using a standard TAP tag protocol (33). The activity of both remodelers was normalized by measuring their effect on the sliding of conventional nucleosomes (34). Nucleosome reconstitution was performed by the salt-dialysis procedure (11). To demonstrate that both reconstituted conventional and H2AL2 nucleosomes contain a full complement of core histones, 5 μg of the nucleosomes reconstituted on 255 bp 601 sequence were run on a 5% native polyacrylamide gel. After completion of the electrophoresis, the bands corresponding to the nucleosomes were excised, eluted overnight in TE buffer, TCA precipitated and analyzed by 18% SDS–PAGE. The gel was stained by Sypro ruby protein gel staining solution from Invitrogen for better sensitivity.

Exonuclease III mapping, footprinting, micrococcal nuclease digestion

Exonuclease mapping, DNase I and hydroxyl radical footprinting were performed as described previously (24,35,36). Micrococcal nuclease digestion was performed at 8 U/ml at 30°C for indicated times as described previously (25).

Nucleosome mobilization and remodeling

Mobilization experiments were carried out using centrally positioned nucleosomes, reconstituted on a 255-bp DNA fragment containing the 601 positioning sequence. The nucleosome samples (5 ng/μl) were incubated in remodeling buffer (10 mM Tris–HCl, pH 7.4, 5% glycerol, 100 μg/ml BSA, 1 mM DTT, 0.02% NP40, 40 mM NaCl, 2.5 mM $MgCl_2$ and 1 mM ATP) with different concentrations of remodelers for 45 min at 30°C and loaded on a 5% native PAGE. End positioned nucleosomes reconstituted on a 200 bp 601 DNA fragment (200 ng) were incubated in remodeling buffer with SWI/SNF and RSC as indicated. The reaction was stopped at different time points (aliquoting) by adding 1 μg of plasmid DNA and 0.02 U of apyrase. These aliquots were subsequently digested by the same amount of DNase I. Similar experiment was done using RSC on the centrally positioned nucleosome with end labeled 601 DNA (Figure 8B).

'One pot' restriction enzyme accessibility assay

For 'one pot' assay 200 ng of core particle nucleosomes were digested with HaeIII with final concentration of 5 U/μl. Aliquots were taken at different time points and the reaction stopped. Phenol chloroform purified and ethanol-precipitated DNA fragments were separated on 8% sequencing PAGE and quantified. The accessibility of different superhelical locations was quantified after normalizing the data against the ratio of different probes in the mixture (31).

Xba 1 restriction assay

To confirm the inefficiency of remodeler to slide the H2Al2 nucleosome, an XbaI restriction site in the linker DNA was probed for eventual inhibition of restriction by the translocation of nucleosomes. Briefly, conventional and H2AL2 nucleosomes were reconstituted on an end-labeled 255 bp centrally positioned 601.2 sequence with 51- and 57-bp linkers. The nucleosomes were subjected to RSC remodeling reaction at 30°C in remodeling buffer lacking glycerol for 45 min and stopped by adding 0.01 units of apyrase. A quantity of 0.04 units/μl of XbaI was added to the reaction mixture and aliquots were taken at different time points and the reaction stopped. The purified DNA was resolved by 8% sequencing gel. Note that under the buffer condition used the maximum XbaI cleavage was below 60%, even on naked DNA.

Atomic force microscopy

AFM imaging of conventional and H2AL2 nucleosomes was carried out as described previously (37). APTES-mica surfaces were used to trap the 3D conformations of the nucleosomes (37). The samples were visualized by using a Nanoscope III AFM (Digital Instruments™, Veeco, Santa Barbara, CA) in Taping mode in air. Automated image analysis was performed using a specially designed Matlab script (The Mathworks, Natick, MA) based on morphological tools, which allowed the precise length measurement for each naked DNA arm from the nucleosome (37).

Centrally positioned nucleosomes, reconstituted on 255 bp 601 sequence, were used in the AFM experiments. The length (L_c) of DNA in complex with the histone octamer was calculated by $L_c = L_{tot} - L_- - L_+$ where L_{tot} is 255 bp, and L_+ and L_- are the long and the short naked DNA arm of the nucleosome, respectively. The position of the nucleosome relative to the center of the DNA was deduced by $\Delta L = (L_+ - L_-)/2$ (37). An 8-bp sliding box was used for the construction of both L_c and ΔL smooth distributions (37).

To study the effect of remodeler, the nucleosomes were incubated with RSC for 30 min at 29°C in a buffer containing 10 mM Tris pH = 7.4, 1.5 mM $MgCl_2$ and 1 mM ATP. A drop of the reaction mixture was diluted and deposited on functionalized mica surface for visualization by AFM. To plot the conventional and variant nucleosome position distribution, only the nucleosomes having their DNA complexed length in the range $<L_c> \pm \sigma L_c$ were selected (where $<L_c>$ and σL_c are, respectively, the mean and the standard deviation of the complexed length distribution in the absence of RSC.

Electron cryo-microscopy

Electron cryo-microscopy samples preparation was performed as described (38). Briefly, the film surface of the electron microscopy grids was treated by subsequent evaporation of carbon and carbon–platinum layers. After dissolving the plastic support, 3 μl of either conventional or H2AL2 tri-nucleosome solution were deposited on the grid, the majority of the liquid was removed by Whatman blotting paper and the grid was then immediately plunged into liquid ethane. The grid was transferred without re-warming in Philips Tecnai G2 Sphera microscope equipped with Ultrascan 1000 CCD camera (Gatan).

RESULTS

Histone H2AL2 is specifically expressed in the testis and could efficiently replace conventional H2A in the nucleosome.

H2AL2 is a recently identified mouse H2A histone variant (23). H2AL2 shows only 41% identity with conventional H2A (23). The protein exhibits similar primary sequence to that of H2A.Bbd, a human variant of H2A (see Figure 1A). Indeed, both H2A.Bbd and H2AL2 show an arginine tract at their N-termini and shorter docking domain than that of H2A (Figure 1A). H2A.Bbd is mainly expressed in testis, but it was also found in other tissues (39,40). RT-PCR data have suggested that H2AL2,

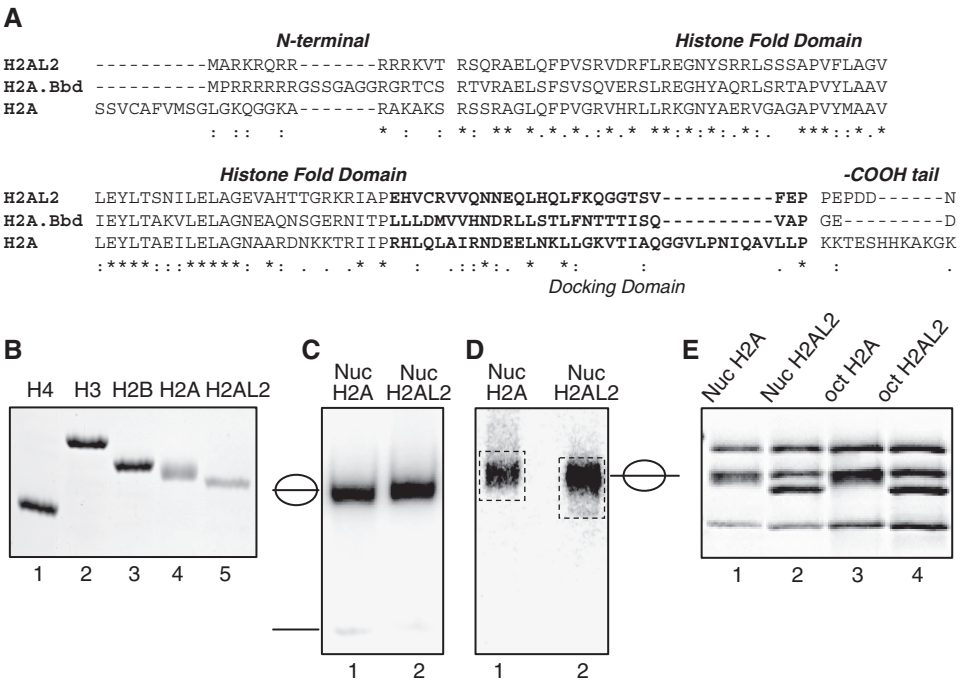

Figure 1. The histone variant H2AL2 can substitute for conventional H2A in the nucleosome. (**A**) Sequence alignment of mouse H2A.1 and H2AL2 and human H2A.Bbd. The N- and C-termini, the histone-fold domain as well as the docking domain (in bold) are indicated. (**B**) SDS PAGE of the purified recombinant histones used for nucleosome reconstitution. (**C**) EMSA of reconstituted nucleosome core particles. ^{32}P-end labeled 147 bp 601.2 DNA sequence was used to reconstitute conventional and histone variant H2AL2 core particles. The reconstituted particles were run on 5% PAGE under native conditions. The positions of the core particles and of free DNA are indicated. Note that under the conditions of reconstitution essentially no free DNA was observed. (**D**) Preparative EMSA of reconstituted nucleosomes. Conventional and H2AL2 nucleosomes, reconstituted on 255 bp 601 DNA sequence, were run on 5% native PAGE, the bands corresponding to the nucleosomes were excised and then the nucleosomes were eluted from the gel. The gel-purified nucleosomes were run on SDS electrophoresis. (**E**) SDS PAGE of both conventional and H2AL2 histone octamers (lanes 3 and 4) and gel-purified reconstituted nucleosomes (lanes 1 and 2).

similarly to H2A.Bbd, was expressed in different tissues, but mainly in testis (23). Since PCR is, however, very sensitive to small contaminations; we have studied the expression of H2AL2 in different mouse tissues by using Northern blot analysis. The data show that, in general agreement with the reported data, H2AL2 is expressed only in testis (see Supplementary Figure 1), suggesting that H2AL2 is a mouse testis-specific histone variant.

H2A.Bbd could be used to reconstitute nucleosomes, but the H2A.Bbd nucleosomes exhibited peculiar properties (25,26,28–30,39). Bearing in mind the primary sequence similarity between H2A.Bbd and H2AL2 one could expect similar behavior of H2AL2 nucleosomes. To test this we first reconstituted H2AL2 nucleosomes (Figure 1). We expressed and purified conventional core histones as well as H2AL2 to homogeneity (Figure 1B) and used them to reconstitute nucleosome core particles by using ^{32}P-end-labeled 147 bp 601.2 positioning sequence. The data show (Figure 1C) no presence of free DNA in the reconstituted both conventional and H2AL2 nucleosomes illustrating that H2AL2, similar to H2A.Bbd, could efficiently replace conventional H2A in the histone octamer.

To further show that the reconstituted particles contain a full complement of core histones, we used conventional and H2AL2 histone variant nucleosomes, reconstituted on 255 bp 601 DNA sequence. Both particles were run on 5% native gel (Figure 1D) and the bands corresponding to the respective particles were excised from the gel. Then we eluted the nucleosomes from the gel slices and separated the histones in 18% SDS–PAGE (Figure 1E). As seen, a full complement of core histones is observed in both cases demonstrating that *bona fide* particles are reconstituted under our experimental conditions.

DNase I and hydroxyl radical footprinting of H2AL2 histone variant nucleosomes

To study the organization of the nucleosomal DNA in the variant H2AL2 particles we have used both DNase I and hydroxyl radical footprinting (Figure 2). Numerous distinct alterations were observed in the DNase I digestion pattern of the H2AL2 nucleosome core particle (Figure 2A, lanes 2–7) compared to that of the conventional core particle (Figure 2A, lanes 9–14). Indeed, changes in the intensity of many bands corresponding to the DNase I digestion products all over the length of the nucleosomal DNA were clearly detected. The OH cleavage pattern of the H2AL2 255-bp nucleosome particle also exhibited some alterations. These alterations were more pronounced towards the end of the DNA complexed with the H2AL2 histone octamer, where the contrast of the bands was clearly decreased (Figure 2B, compare lanes

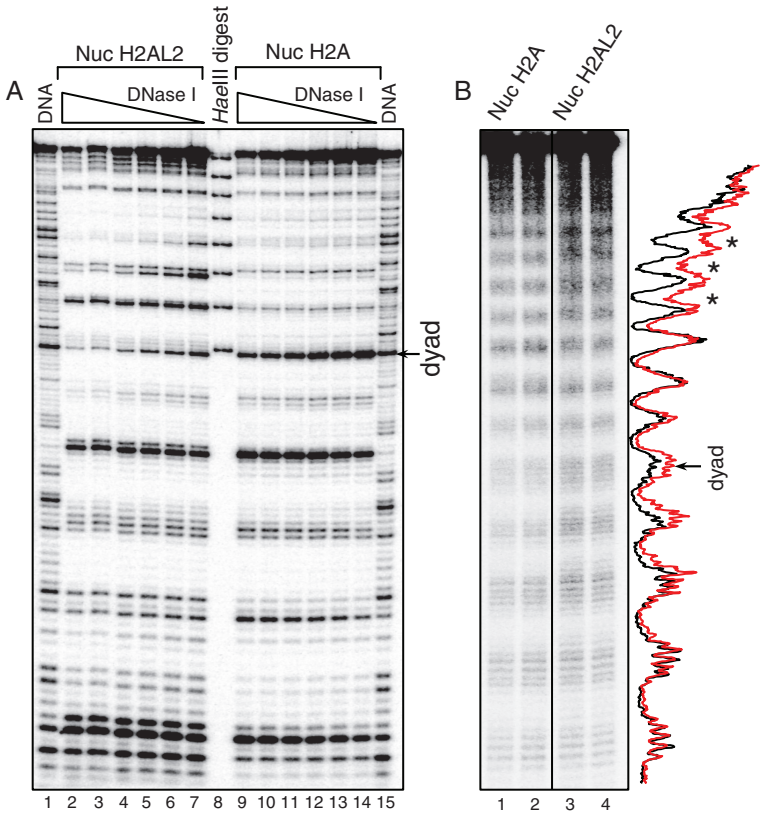

Figure 2. DNase I and hydroxyl radical footprinting show alterations in the structure of the histone variant H2AL2 nucleosome. (**A**) DNase I footprinting. Conventional (lanes 2–7) and H2AL2 (lanes 9–14) nucleosome core particles were reconstituted by using ^{32}P-radiolabeled 147 bp 601.2 positioning DNA sequence and digested with decreasing amount of DNase I. After purification, the cleaved DNA was run on an 8% sequencing PAGE. Lanes 1 and 15 show the DNase I digestion pattern of free DNA. The molecular marker (lane 8) is a HaeIII digested mix of the eight 147 bp 601.2 fragments; the band with the highest molecular weight corresponds to 147 bp and the consecutive bands are separated by 10 bp (see 'Material and Methods' section, one pot assay). The position of the nucleosome dyad is indicated at the right part of the figure. (**B**) Hydroxyl radical footprinting. Centrally positioned conventional and H2AL2 nucleosomes were reconstituted on ^{32}P-radiolabeled 255 bp 601 positioning DNA sequence and subjected to OH cleavage. The cleaved DNA was purified from the conventional and H2AL2 nucleosomes and run (in duplicate) on 8% PAGE under denaturing conditions. Lanes 1 and 2 were not adjacent to lanes 3 and 4 in the original gel, and they were thus demarked accordingly. The right part of the figure shows the scans of the OH cleavage patterns of the two samples (red, H2AL2 nucleosomes; black, H2A nucleosomes). The position of the nucleosome dyad is indicated. Note the lower contrast of the cleaved H2AL2 nucleosomal DNA (designated by asterisk) toward the end of the nucleosome DNA.

3 and 4 with lanes 1 and 2). We attributed these changes in the DNase I and OH cleavage patterns to reflect H2AL2-associated perturbations in the overall structure of the variant nucleosome.

Micrococcal and exonuclease III digestion demonstrates a distinct organization of the H2AL2 nucleosome

The structure of the H2AL2 nucleosomes was further investigated by micrococcal nuclease and exonuclease III digestion. For the experiments with micrococcal nuclease, a 255 bp 601 sequence was ^{32}P-body labeled and used for reconstitution of both conventional and H2AL2 nucleosomes. These nucleosomes were centrally positioned leaving two free DNA arms of 52 and 56 bp, respectively. Identical amounts (~50 ng) of these two samples were incubated in the presence of 1 μg of naked DNA (the presence of nearly 20-fold excess of naked DNA allows a very precise standardization of the digestion conditions; note that under these conditions the nucleosomes are stable and no transfer of histones to the naked DNA was observed) for the indicated times with 8 units/ml of micrococcal nuclease and after arresting the digestion, DNA was isolated and run on a 10% PAGE under native conditions (Figure 3A). In the case of conventional particles, the free DNA arms were rapidly digested and a stable digestion intermediate, corresponding to the core particle, is generated (Figure 3A, lanes 2–6). Note that even at the longest time of digestion (32 min, Figure 3A) a very weak subnucleosomal digestion band was detected. The H2AL2 particles show, however, different digestion pattern (Figure 3A, lanes 8–12). Indeed, a strong band corresponding to the subnucleosomal particle was already observed at 8 min of digestion and at the longest time of digestion (32 min) essentially only subnucleosomal particles were generated. This demonstrates that the H2AL2 nucleosomal DNA is more accessible to micrococcal nuclease suggesting that its structure is more relaxed compared to that of the conventional particle.

The accessibility of H2AL2 reconstituted nucleosomal arrays to micrococcal nuclease was also investigated and was compared to that of conventional nucleosomal arrays

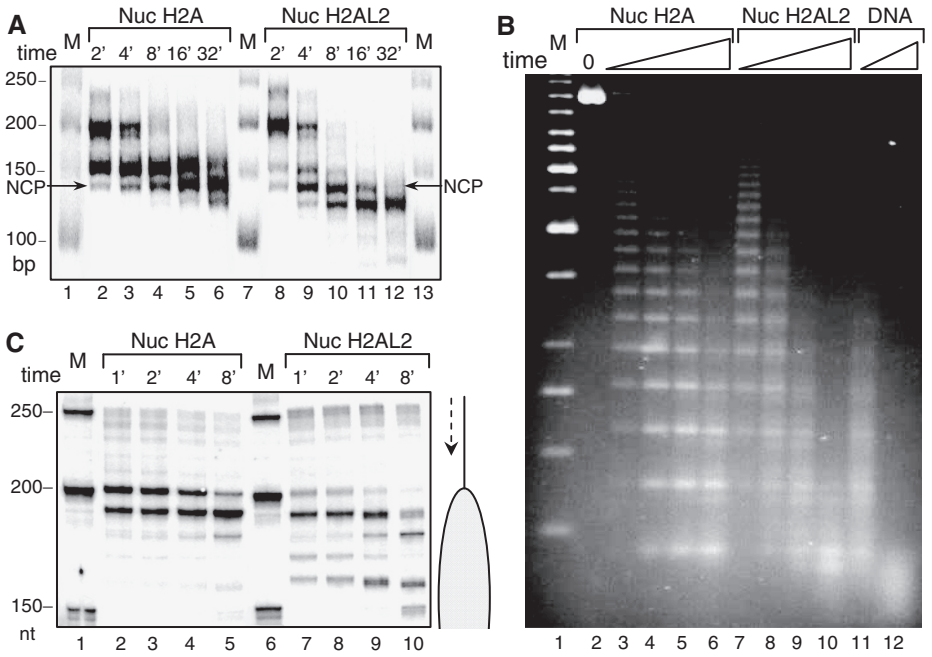

Figure 3. Higher accessibility of H2AL2 mono-nucleosomes and nucleosomal arrays to micrococcal nuclease and exonuclease III digestion. (**A**) Identical amounts (50 ng) of conventional (Nuc H2A) and H2AL2 (Nuc H2AL2) nucleosomes (reconstituted on a body-labeled 255 bp 601 sequence) in a solution of 10 µl were digested (in the presence of 1 µg plasmid DNA) with 8 units/ml of micrococcal nuclease for the indicated times (2–32 min) at room temperature. After arresting the reaction, the digested DNA was isolated and run on 10% native PAGE. Lanes 1, 7 and 13, DNA molecular mass markers. The lengths (in bp) of the markers are indicated at the left side of the figure. (**B**) Micrococcal nuclease digestion of conventional H2A and histone variant H2AL2 33X200–601 arrays. Hundred nanogram of fully saturated reconstituted conventional (lanes 2–5), H2AL2 (lanes 7–10) and naked DNA (lanes 11 and 12) arrays were digested for different time points with micrococcal nuclease. The digested DNA was isolated and run on 1.4% agarose gel and visualized with SYBR green. Lane 1, 1-kb molecular mass DNA marker. (**C**) Exonuclease III digestion of conventional and H2AL2 nucleosomes. Fifty nanogram of uniquely 5′-end-labeled centrally positioned nucleosomes (reconstituted on a 255 bp 601 sequence) were digested with the same amount of exonuclease III for the times indicated. The reaction was arrested and, after purification, the digestion products were run on an 8% denaturing gel. The lengths of the 50-bp DNA marker (lanes 1 and 6) are indicated at the left side of the figure.

(Figure 3B). The data clearly show that, as in the case of mononucleosomes, the H2AL2 arrays are more rapidly digested than the conventional ones indicating that not only the monosomes but also the nucleosomal H2AL2 arrays exhibited more relaxed structure.

The accessibility of H2AL2 nucleosomes to exonuclease III was also studied. These experiments use a centrally positioned nucleosome reconstituted on a ^{32}P-5′end-labeled 255 bp 601 DNA sequence. This nucleosome bears, as mentioned above, two free DNA 'arms' of 52 and 56 bp, respectively. Incubation of the conventional nucleosomes with exonuclease III results into two major stable intermediates: a first one, located at position 200 bp, and thus corresponding to the border of the particle (Figure 3C, lanes 2–5) and a second one at around 185 bp position and reflecting an arrest of the nuclease in the interior of the particle. Small amounts of lower molecular weight intermediates are also generated at longer times of incubation with the enzyme. Upon increasing the time of digestion the amount of the first intermediate decreases, that of the second increases, but even at the longest time of digestion the first intermediate is still present. The exonuclease III digestion profile of the H2AL2 particle was totally different from that of the conventional one, since six distinct digestion products were produced (Figure 3C, lanes 7–10), the molecular masses of the first three higher molecular bands being the same as those of the conventional particles. Increasing the time of digestion leads to the generation of mainly lower molecular mass fragments, corresponding to pauses of the exonuclease deeply in the interior of the H2AL2 particle. The observed ability of exonuclease III to overcome the structural barriers imposed by the H2AL2 particle evidences for weaker histone–DNA interactions, and thus for weaker stability of this particle.

The 'one pot assay' shows that the interactions between the histone octamer and the ends of nucleosomal DNA are highly perturbed within the H2AL2 particle

To further study the structure of the H2AL2 histone variant nucleosome we also used a recently described 'one pot assay' (31). Briefly, both conventional and H2AL2 147-bp core particles were reconstituted by using eight mutated ^{32}P-end-labeled 601.2 DNA sequences. Each individual sequence was mutated in a way to introduce a single Hae III restriction site in it. All restriction sites exhibit the same rotational position with an outward-facing minor groove and are separated by 10 base pairs (31)

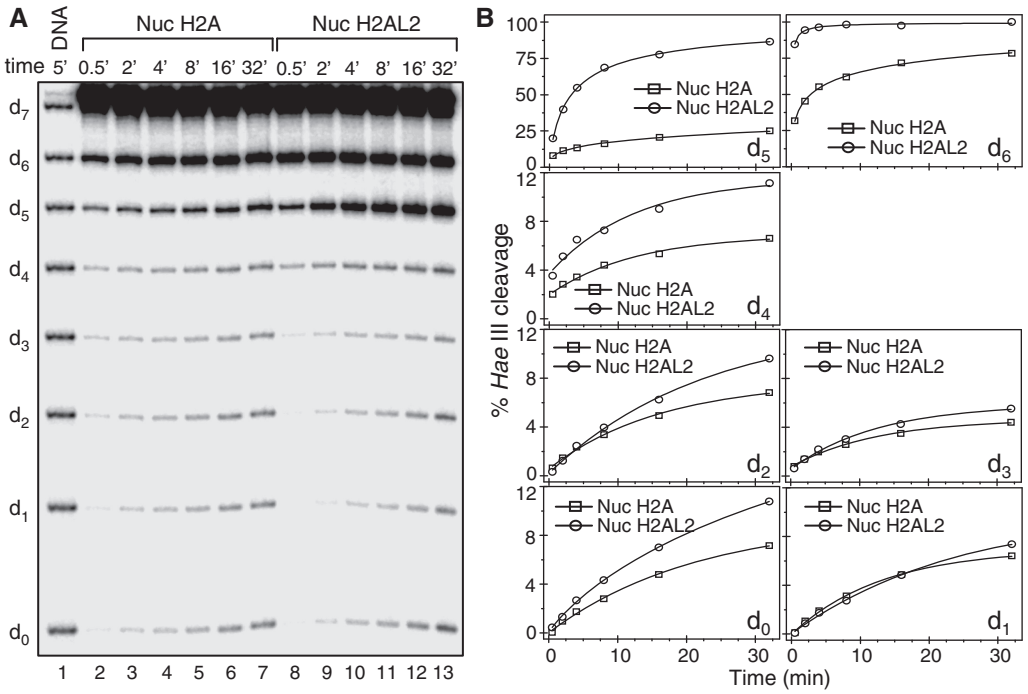

Figure 4. 'One pot assay' of conventional and H2AL2 nucleosomes. (**A**) Kinetics of the HaeIII digestion of conventional H2A (Nuc H2A) and variant H2AL2 (Nuc H2AL2) nucleosomes. Identical amounts of both types of nucleosomes were digested with 5 U/μl of Hae III at 30°C for the times indicated. After arresting the digestion, DNA was isolated and run on an 8% denaturing PAGE. Lane 1, naked DNA digested with 5 U/μl for 5 min. (**B**) Quantification of the data presented in (**A**). Note that the quantification for the accessibility at d_7 is not presented, since the corresponding band is not resolved from the undigested DNA under our conditions (see *panel* A).

[for simplicity further in the text the Hae III restriction sites will be designated as d_0 (superhelical position 0) to d_7 (superhelical position 7)]. Then, the nucleosome samples were incubated with 5 units/μl of Hae III for increasing times. After arresting the reaction, DNA was isolated and run on 8% PAGE under denaturing conditions (Figure 4A). The quantification of the HaeIII cleavage efficiency at the different sites is shown at Figure 4B. As seen, major differences in the cleavage efficiencies are observed at d_5 and d_6, i. e. close to the end of the nucleosomal DNA (note that under our experimental conditions we were unable to separate the HaeIII d_7 cleavage products from the non-cleaved fragments, which did not allow the calculation of the cleavage efficiency at d_7). Indeed, both the initial rate of cleavage (the slope of the curves) as well as the saturation of the cleavage are much higher for these superhelical positions for the H2AL2 nucleosomes compared to those of the conventional ones. We conclude that the histone–DNA interactions at the end of the nucleosomal DNA are strongly perturbed within the H2AL2 particle. Note that there are also differences inside the nucleosome, particularly at d_0, d_2 and d_4 consistent with the DNase I digestion data as seen in figure 2.

AFM imaging of conventional and H2AL2 nucleosomes

The described structural alterations in the H2AL2 nucleosomes are similar to those of the H2A.Bbd nucleosomes (25). The length (L_c) of the DNA complexed with the histone octamer was found to be only ~130 bp within the H2A.Bbd nucleosome (25). With this in mind, we next asked whether the H2AL2 variant histone octamer exhibited the same property, i.e. whether it also organizes less DNA than the conventional octamer does (147 bp). To this end, we imaged both centrally positioned conventional and H2AL2 nucleosomes reconstituted on 255 bp 601 DNA fragment (Figure 5A and B). The relatively long free DNA arms present at each end of the nucleosome allowed their precise length measurement by AFM image analysis. This allowed, in turn, the calculation of both the length of the DNA complexed with the histone octamer L_c ($L_c = L_{tot} - L_+ - L_-$, where $L_{tot} = 255$ bp is the length of the 601 fragment used for reconstitution, L_+ and L_- are the lengths of the long and the short DNA arms, respectively, as measured by AFM image analysis) and the position of the nucleosome relative to the DNA template center $\Delta L = (L_+ - L_-)/2$ [Figure 5C, D and (37)]. The measurements were performed in a large number of objects ($N = 1252$ conventional and $N = 2805$ H2AL2 nucleosomes), which made them statistically relevant. The mean of the length distribution for DNA complexed with the conventional histone octamer was located close to 145 bp and interestingly around 130 bp, for the variant H2AL2 nucleosome (Figure 5C). The position of the nucleosome relative to the DNA center, $\triangle L$, was the same for both particles (Figure 5D).

Electron cryo-microscopy shows a very open structure of the H2AL2 tri-nucleosomes

The perturbation of the histone–DNA interactions at d_5–d_6 and the ability of the H2AL2 octamer to organize

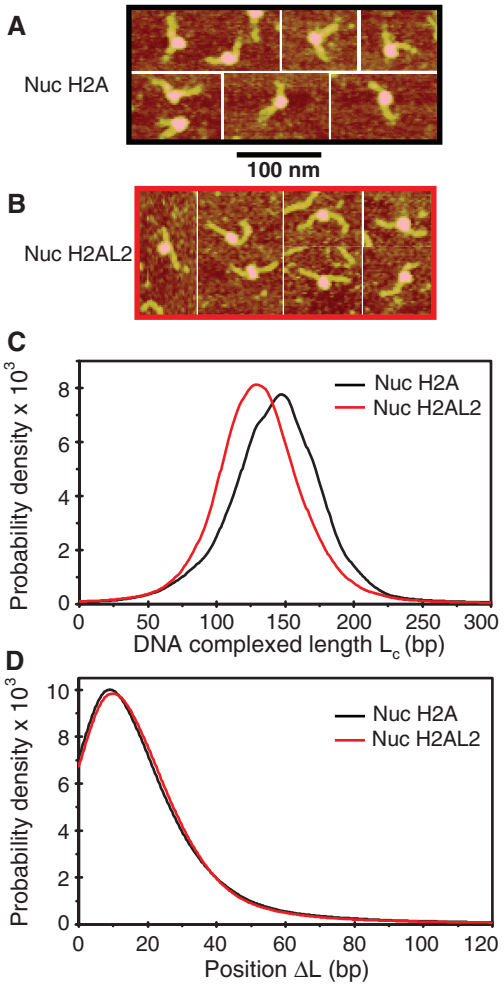

Figure 5. AFM imaging shows that the H2AL2 histone octamer is complexed with ~130 bp of DNA. Centrally positioned conventional and H2AL2 nucleosomes were reconstituted on 255 bp 601 DNA sequence and visualized by AFM. Representative AFM images for the conventional (nuc H2A) and H2AL2 (nuc H2AL2) particles are presented in (**A**) and (**B**), respectively. (**C**) Complexed DNA length (L_c) distribution for conventional and H2AL2 nucleosomes. Note the difference in the peak position in the distribution curves of the two samples. (**D**) Nucleosome position (ΔL) distribution for conventional and H2AL2 nucleosomes. The numbers of particles used for the calculation of the distributions were N = 1252 and N = 2805 for conventional and H2AL2 nucleosomes, respectively.

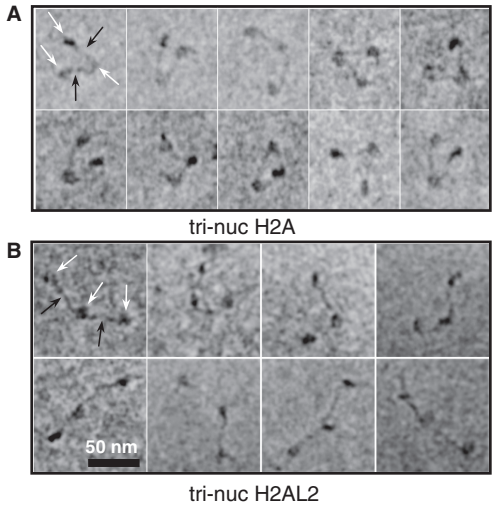

Figure 6. Electron cryo-microscopy visualization of conventional H2A and histone variant H2AL2 tri-nucleosomes. A DNA fragment containing three tandem 601 positioning sequence repeats was used to reconstitute conventional (**A**) and H2AL2 tri-nucleosomes (**B**) and they were visualized by E-CM. Typical micrographs for both types of particles are shown. The conventional trinucleosomes exhibit V-shaped structure with the two-end nucleosomes at both ends of the 'V' and the middle nucleosome at the center of the 'V'. In contrast, the majority of the H2AL2 trinucleosomes exhibit 'beads on a string' structure and very few H2AL2 trinucleosomes show open 'V'-type of organization. Black arrows indicate the linker DNA, while the nucleosome is designated by white arrows.

only ~130 bp may affect the entry/exit angle of the nucleosomal DNA ends. To test this we have used electron cryo-microscopy (EC-M). E-CM experiments are performed in vitrified solutions without the utilization of any contrasting reagents, which allows the visualization of the 'native', unperturbed structure of the samples. E-CM was very successfully used for investigating the structure of both reconstituted conventional and H2A.Bbd histone variant nucleosomes (25) as well as native oligosomes and high molecular weight chromatin samples (41). Note that the trinucleosomes are of particular interest for studying the linker orientation (42). With this in mind, we have reconstituted precisely positioned 601 conventional and H2AL2 trinucleosomes and visualized them by E-CM (Figure 6). The conventional trinucleosomes exhibited a typical 'V' (equilateral triangle) shape with two nucleosomes located at each end of the trinucleosomal DNA and the middle nucleosome at the 'point' of the 'V' (Figure 6A). The 3D organization of the H2AL2 trinucleosomes was, however, quite different (Figure 6B). Typically, the H2AL2 trinucleosome shows 'beads on a string' organization, and in some cases, a very open 'V' type organization with the linker DNAs forming a very large angle (Figure 5B). We conclude that the variant H2AL2 octamer cannot properly organize the 3D conformation of the entry/exit nucleosomal DNA. We attribute this to the altered interactions of the entry/exit ends of nucleosomal DNA with the H2AL2 histone variant octamer.

The presence of H2AL2 affected both RSC and SWI/SNF nucleosome remodeling and mobilization

The data described above unequivocally demonstrate that the incorporation of H2AL2 in the nucleosomes results in perturbation of their structure. Perturbation in the nucleosome structure induced by the presence of the histone variant H2A.Bbd led to inhibition of both nucleosome remodeling and mobilization (25,28). This prompted us to next ask if H2AL2, as H2A.Bbd, interferes with nucleosome remodeling and mobilization. DNase I footprinting assay was used for studying the capacity of RSC and SWI/SNF to remodel the nucleosomes. Conventional and H2AL2 end-positioned nucleosomes were reconstituted on ^{32}P-end-labeled 200 bp 601 DNA sequence. Identical amounts of both samples were incubated for different times (from 2.5 to 40 min) at 30°C with either RSC or SWI/SNF. After arresting the remodeling reaction, the

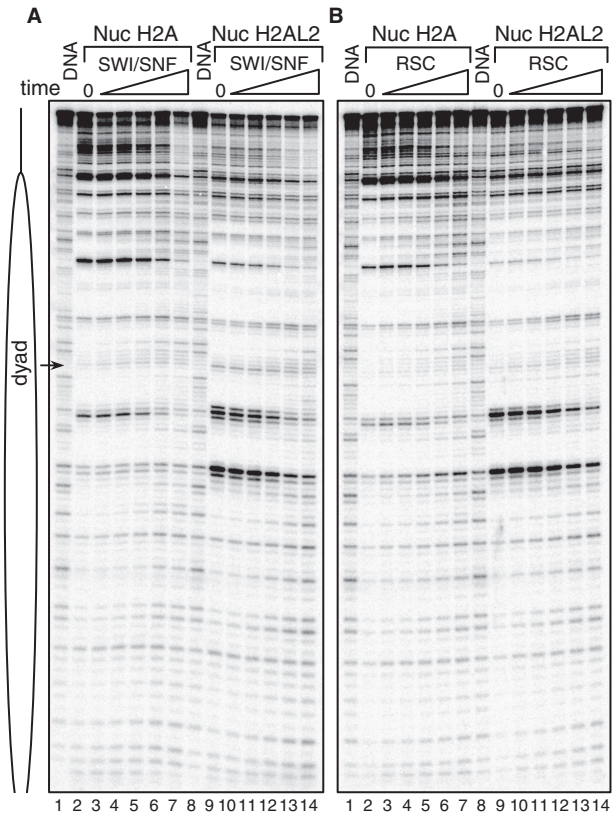

Figure 7. SWI/SNF and RSC remodeling of conventional and H2AL2 nucleosomes. End-positioned conventional (lanes 2–7) and H2AL2 (lanes 9–14) nucleosomes were reconstituted on a ^{32}P-5′-labeled 200 bp 601 DNA fragment and incubated for increasing times (from 2.5 to 40 min) at 30°C with two units of either SWI/SNF (**A**) or RSC (**B**). After arresting the reactions, the samples were digested with DNase I, DNA was extracted and run on an 8% sequencing gel. The position of the dyad is indicated at the left part of the figure. Lanes 1 and 8 of each *panel* show the digestion pattern of free DNA.

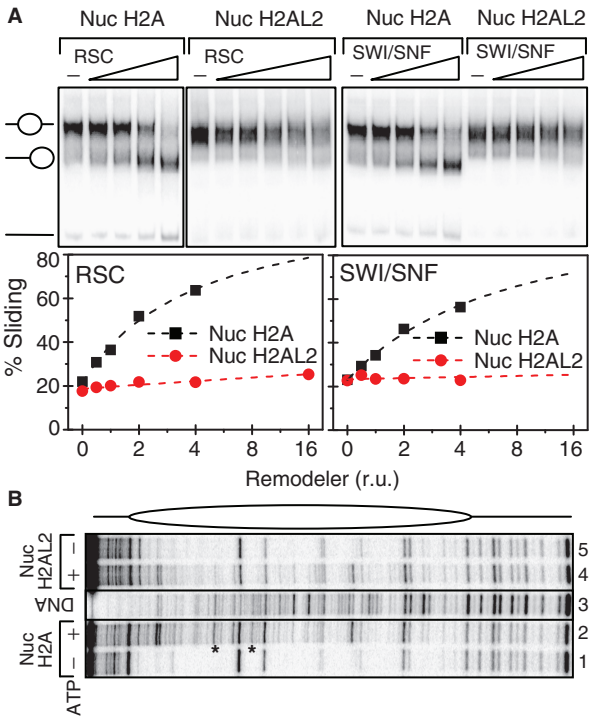

Figure 8. The presence of H2AL2 interferes with both SWI/SNF and RSC nucleosome remodeling and mobilization. (**A**) Nucleosome mobilization assay. Centrally positioned conventional and H2AL2 nucleosomes were reconstituted on a ^{32}P-end-labeled 255 bp 601 DNA fragment and used for either RSC (left panel) or SWI/SNF (right panel) mobilization assay. Both types of reconstituted nucleosomes were incubated for 40 min at 30°C with increasing amounts of the respective remodeler in the presence of ATP. After arresting the reaction, the samples were run on a 5% native PAGE (the conventional and H2AL2 RSC-treated nucleosomes were run on two different gels and the data are presented in two separate panels). The center and the end-positioned (slid) nucleosomes and free DNA are indicated. The lower part of the figure shows the quantification of the data. (**B**) DNase I footprinting of RSC remodeled conventional and H2AL2 nucleosomes. Both centrally positioned conventional and H2AL2 particles, reconstituted on a ^{32}P-end-labeled 255 bp 601 DNA fragment, were treated with the highest amount of RSC used in the mobilization reaction as described in (A). After arresting the remodeling reaction the samples were digested with DNase I, the cleaved DNA was purified and run on an 8% sequencing PAGE. A schematic of the nucleosome is shown in the upper part of the figure. Lane 3, showing the digestion of the naked DNA, was not adjacent to lanes 2 and 4 in the original gel, and was thus demarked accordingly.

samples were treated with DNase I, the digested DNA was purified and run on 8% PAGE under denaturing conditions. SWI/SNF (Figure 7A) and RSC (Figure 7B) remodeled both conventional and H2AL2 nucleosomes. The 10-bp DNase I nucleosomal repeat was lost and many bands corresponding to the respective bands of the digestion of free DNA were observed (Figure 7A and B, compare lanes 2–7 with lanes 9–14). However, both RSC and SWI/SNF remodeled about 2.5 times more efficiently the conventional particles as determined by quantification of the intensity of some specific bands (results not shown). We conclude, that the presence of H2AL2, similarly to that of H2A.Bbd (25,28), interferes with nucleosome remodeling.

Is H2AL2 able to affect nucleosome mobilization? To test this we have carried out a standard nucleosome mobilization assay. Centrally positioned conventional and H2AL2 nucleosomes were reconstituted by using ^{32}P-end-labeled 255 bp 601 fragment and incubated for 45 min (in the presence of ATP) with increasing amount of either RSC or SWI/SNF (Figure 8). Treatment with the remodelers resulted, as expected, in loss of the 10-bp repeat in the DNase I digestion pattern of either one of the particles (Figure 8B). However, careful comparison of the remodeled patterns (lanes 2 and 4 in Figure 8B) shows again some differences. Indeed, the remodeling of the conventional nucleosomes was stronger compared to that of the variant particles. In addition, some bands present in the digestion pattern of remodeled conventional nucleosomes were not detected in the digestion pattern of remodeled H2AL2 nucleosomes (Figure 8B, bands marked by stars). These results are in agreement with the data presented in Figure 7 for the 200-bp H2AL2 nucleosome and evidence for a less-efficient remodeling of the variant H2AL2 255 bp particle.

Under the conditions of the experiments both remodelers induced a relocation of conventional nucleosomes

(Figure 8A). Although, neither RSC nor SWI/SNF was able to relocate efficiently the H2AL2 histone variant octamer to the end of the nucleosomal DNA (Figure 8A). Quantification of the data showed that the efficiency (the initial slope of the curves, Figure 8A, lower panels) of the variant H2AL2 histone octamer relocation at the end of the nucleosomal DNA by either one of the remodelers was at least 10-fold lower than that of the conventional histone octamer. Note, however, that the upper band corresponding to the centrally positioned H2AL2 nucleosomes is becoming larger upon incubation with higher amounts of either RSC or SWI/SNF (Figure 8A). This might be associated with some heterogenization due to either histone–DNA contacts disruption and/or short range relocation of the H2AL2 particles.

We have also studied the capacity of RSC to mobilize H2AL2 nucleosomes by using an enzyme restriction assay (see schematics of the assay, Figure 9A). We have first incubated both conventional and H2AL2 nucleosomes with an amount of RSC sufficient to relocate the conventional nucleosomes at the end of the nucleosomal DNA (see Figure 8A). After arresting the reaction, both types of nucleosomes were digested with Xba 1, whose restriction site is located in the linker DNA at 233 bp from the ^{32}P-labeled end of the nucleosomal DNA. If the nucleosomes were mobilized by RSC (in the presence of ATP) one should expect the yield of cleavage to drop two-fold (see Figure 9A). This was really the case for conventional nucleosomes (Figure 9B and C). In contrast, essentially no change in the Xba 1 cleavage yield for the RSC incubated H2AL2 nucleosomes was detected (Figure 9B and C). These data combined with the EMSA results (Figure 8A) demonstrate that the presence of H2AL2 interferes with the chromatin remodeler induced relocation of the variant particles at the end of the nucleosomal DNA. This conclusion was further supported by studying the RSC-induced mobilization by AFM (Figure 9D). The AFM imaging showed that treatment with RSC generated conventional, but essentially not H2AL2, end-positioned nucleosomes (Figure 9D).

DISCUSSION

In this work, we have studied the structural and functional properties of the histone variant H2AL2 nucleosomes. We confirmed that this histone variant is testis-specific and we show that it can efficiently replace conventional H2A in the nucleosome. The variant H2AL2 nucleosome exhibited both structural and functional properties distinct from those of the conventional ones. DNase I and OH footprinting, micrococcal nuclease and exonuclease III digestion and nucleosomal DNA restriction nuclease accessibility assay demonstrated alterations in the overall H2AL2 nucleosome structure. AFM imaging showed that only ~130 bp of DNA were wrapped around the H2AL2 histone variant octamer. The H2AL2 trinucleosomes exhibited essentially 'beads on a string' nucleosomal organization in contrast to the conventional trinucleosomes, which showed equilateral triangle shape. Finally, we found that H2AL2 nucleosomes cannot be efficiently

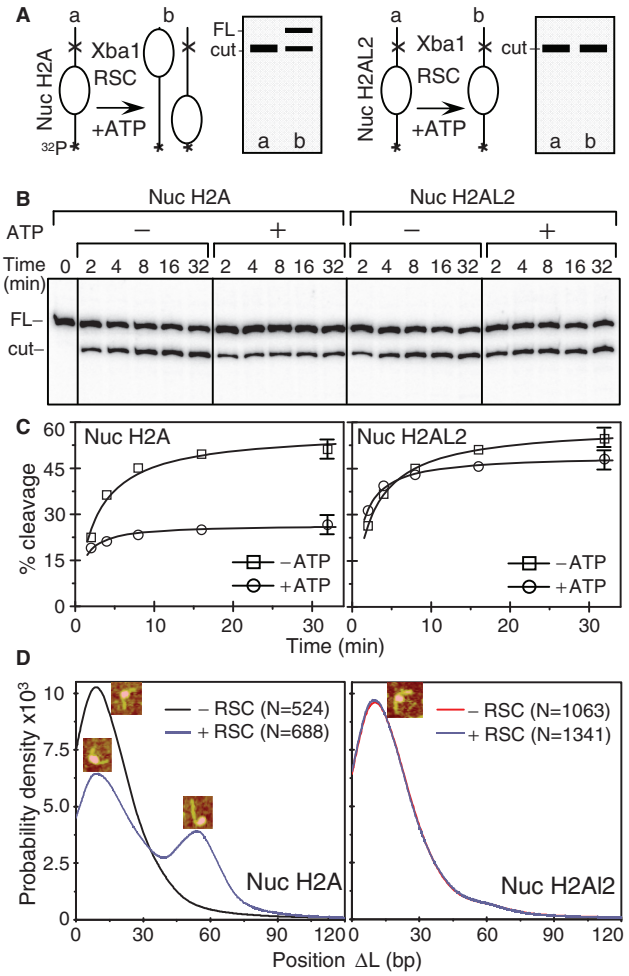

Figure 9. XbaI nuclease restriction and AFM analyses of the RSC-induced relocation of conventional and histone variant H2AL2 nucleosomes. (**A**) Schematics of the XbaI restriction analysis used to study the RSC-induced mobilization of conventional and histone variant H2AL2 nucleosomes. The XbaI restriction site is located in the linker DNA of the nucleosome at 233 bases from the end of the ^{32}P-end-labeled 601.2 DNA fragment. If RSC induces sliding of the nucleosome, the cut efficiency of XbaI is expected to decrease two-fold (the nucleosome will be mobilized to both ends of the DNA fragment, left panel). If RSC is unable to mobilize the nucleosome, no decrease of the XbaI cut efficiency will be observed (right panel). (**B**) Identical amounts (150 ng) of H2A (left panel) or H2AL2 (right panel) ^{32}P-end-labeled nucleosomes were incubated with 0.04 units/μl of XbaI either in the presence or the absence of 1 mM ATP. After digestion for the times indicated, the reaction was stopped and the digestion products were separated on the same 8% sequencing gel (the migrated products, which loading was not adjacent in the original gel, are demarked by vertical lines). The positions of the full length (FL) and cut DNA fragment are indicated on the left of the figure. (**C**) Quantifications of the data presented in (**B**). Note the 2-fold decrease of cut yield for the conventional H2A nucleosomes (Nuc H2A, left panel) and the absence of effect on the cut yield in the case of H2AL2 (Nuc H2AL2, right panel) nucleosomes. The digestion with Xba 1 was carried out in remodeling buffer and under these conditions a digestion plateau was reached at ~50–60%. (**D**) Position distribution (ΔL) of conventional and H2AL2 histone variant nucleosomes before and after treatment with RSC. Either conventional or H2AL2 nucleosomes were treated with RSC in the presence of ATP and the samples were visualized by AFM. The insets indicate the centrally positioned (first peak) and the mobilized, end-positioned conventional nucleosomes (second peak). The numbers of analyzed nucleosomes are: N(H2A-RSC) = 524, N(H2A + RSC) = 688 conventional nucleosomes and N(H2AL2-RSC) = 1063 and N(H2AL2 + RSC) = 1341 variant nucleosomes, respectively.

both remodeled and relocated at the end of the nucleosomal DNA by either one of the chromatin remodelers RSC or SWI/SNF. The effect of H2AL2 on the efficiency of nucleosome relocation was, however, more pronounced than that on the efficiency of nucleosome remodeling. Note that for the reconstitution of the nucleosomal samples we have used *Xenopus laevis* core histones H2B, H3 and H4, but their mouse analogs are essentially the same, and thus the described results would not be affected.

The above-summarized data indicate that the observed perturbations in the H2AL2 nucleosome structure were sufficient to induce an impediment of the remodeling of the nucleosome and the relocation of the variant histone octamer to the nucleosomal DNA end. In particular, the alterations in the wrapping of DNA around the H2AL2 variant histone octamer may not allow the proper binding of the variant particle in the nucleosome-binding pocket (43–45) of both RSC and SWI/SNF.

H2AL2 is a testis-specific histone variant [(23) and this work]. H2A.Bbd is also expressed mainly in testis. Common properties of the H2AL2 and H2A.Bbd particles are their altered structures and their capacity to interfere with the remodelers' function, i.e. to interfere with nucleosome remodeling and relocation. Therefore, both histones would be involved in the *in vivo* 'construction' of distinct nucleosomes with specialized functions. These functions would require an easier removal of the variant dimers from the nucleosome and no nucleosome mobilization.

We have reported earlier that the docking domain of H2A.Bbd is required for nucleosome mobilization (25). Since the docking domain of H2AL2 differed considerably from that of the conventional H2A and its length is closer to that of H2A.Bbd (see Figure 1A), this indicates that the cells in both mouse and human use very similar strategies to generate nucleosomes lacking the ability to be mobilized by chromatin remodelers.

The H2A.Bbd nucleosomes exhibited an open structure (25). The H2AL2 trinucleosomes also showed an open (beads on a string type) structure and micrococcal nuclease digestion of H2AL2 nucleosome arrays suggest a more relaxed organization of these variant arrays. This appeared to be determined by the altered interactions of the H2AL2 histone octamer with the ends of the nucleosome DNA (this work). Since for the H2A.Bbd the docking domain was required for the generation of the open nucleosome structure we hypothesize that the H2AL2-altered docking domain is also involved in the generation of the open structure of the H2AL2 nucleosomes and nucleosomal arrays. This open structure of both H2A.Bbd and H2L2A chromatin filaments could play an important role during different spermiogenesis-specific processes, including replacement of these histone variants.

SUPPLEMENTARY DATA

Supplementary Data are available at NAR Online.

ACKNOWLEDGEMENTS

We thank Dr Workman for kindly providing us with the yeast strain expressing tagged RSC and SWI/SNF and Dr Daniela Rhodes for providing the 601 chromatin template DNA. We thank Fabien Montel for setting up the automated AFM image analysis. S.D. acknowledges the Franco-Indian scientific program ARCUS for support.

FUNDING

INSERM and CNRS; La Ligue Nationale Contre le Cancer (Equipe labelisé La Ligue to S.D.) the Association pour la Recherche sur le Cancer (Grant N 4821 to D.A.); the Région Rhône-Alpes (Convention CIBLE 2008 to D.A. and S.D.); Agence Nationale de la Recherche (Grant Blanc 'CHROREMBER' to S.D., D.A. and J.B) and the Grant Agency of the Czech Republic (Grant #304/05/2168 to J.B.) and the Ministry of Education, Youth and Sports (Grants MSM0021620806 and LC535 to J.B.) and the Academy of Sciences of the Czech Republic (Grant #AV0Z50110509 to J.B.). Funding for open access charge: Association pour la Recherche sur le Cancer (Grant 4821).

Conflict of interest statement. None declared.

REFERENCES

1. Arents,G., Burlingame,R.W., Wang,B.-C., Love,W.E. and Moudrianakis,E.N. (1991) The nucleosomal core histone octamer at 3.1 A resolution: a tripartite protein assembly and a left-handed superhelix. *Proc. Natl Acad. Sci. USA*, **88**, 10148–10152.
2. Arents,G. and Moudrianakis,E.N. (1995) The histone fold: a ubiquitous architectural motif utilized in DNA compaction and protein dimerization. *Proc. Natl Acad. Sci. USA*, **92**, 11170–11174.
3. Luger,K., Mäder,A.W., Richmond,R.K., Sargent,D.F. and Richmond,T.J. (1997) Crystal structure of the nucleosome core particle at 2.8 Å resolution. *Nature*, **389**, 251–260.
4. Huynh,V.A., Robinson,P.J. and Rhodes,D. (2005) A method for the in vitro reconstitution of a defined "30 nm" chromatin fibre containing stoichiometric amounts of the linker histone. *J. Mol. Biol.*, **345**, 957–968.
5. Robinson,P.J., An,W., Routh,A., Martino,F., Chapman,L., Roeder,R.G. and Rhodes,D. (2008) "30 nm" chromatin fibre decompaction requires both H4-K16 acetylation and linker histone eviction. *J. Mol. Biol.*, **381**, 816–825.
6. Robinson,P.J., Fairall,L., Huynh,V.A. and Rhodes,D. (2006) EM measurements define the dimensions of the "30-nm" chromatin fiber: evidence for a compact, interdigitated structure. *Proc. Natl Acad. Sci. USA*, **103**, 6506–6511.
7. Routh,A., Sandin,S. and Rhodes,D. (2008) Nucleosome repeat length and linker histone stoichiometry determine chromatin fiber structure. *Proc. Natl Acad. Sci. USA*, **105**, 8872–8877.
8. Smirnov,I.V., Dimitrov,S.I. and Makarov,V.L. (1988) NaCl-induced chromatin condensation. Application of static light scattering at 90 degrees and stopped flow technique. *J. Biomol. Struct. Dyn.*, **5**, 1127–1134.
9. Ausio,J., Dong,F. and van Holde,K.E. (1989) Use of selectively trypsinized nucleosome core particles to analyze the role of the histone "tails" in the stabilization of the nucleosome. *J. Mol. Biol.*, **206**, 451–463.
10. Gordon,F., Luger,K. and Hansen,J.C. (2005) The core histone N-terminal tail domains function independently and additively during salt-dependent oligomerization of nucleosomal arrays. *J. Biol. Chem.*, **280**, 33701–33706.
11. de la Barre,A.E., Angelov,D., Molla,A. and Dimitrov,S. (2001) The N-terminus of histone H2B, but not that of histone H3 or its

phosphorylation, is essential for chromosome condensation. *EMBO J.*, **20**, 6383–6393.
12. Scrittori,L., Hans,F., Angelov,D., Charra,M., Prigent,C. and Dimitrov,S. (2001) pEg2 aurora-A kinase, histone H3 phosphorylation, and chromosome assembly in Xenopus egg extract. *J. Biol. Chem.*, **276**, 30002–30010.
13. Wang,G.G., Allis,C.D. and Chi,P. (2007) Chromatin remodeling and cancer, Part I: Covalent histone modifications. *Trends Mol. Med.*, **13**, 363–372.
14. Ausio,J. and van Holde,K.E. (1986) Histone hyperacetylation: its effects on nucleosome conformation and stability. *Biochemistry*, **25**, 1421–1428.
15. Garcia-Ramirez,M., Rocchini,C. and Ausio,J. (1995) Modulation of chromatin folding by histone acetylation. *J. Biol. Chem.*, **270**, 17923–17928.
16. Shogren-Knaak,M., Ishii,H., Sun,J.M., Pazin,M.J., Davie,J.R. and Peterson,C.L. (2006) Histone H4-K16 acetylation controls chromatin structure and protein interactions. *Science*, **311**, 844–847.
17. Strahl,B.D. and Allis,C.D. (2000) The language of covalent histone modifications. *Nature*, **403**, 41–45.
18. Bao,Y. and Shen,X. (2007) SnapShot: chromatin remodeling complexes. *Cell*, **129**, 632.
19. Côté,J., Peterson,C.L. and Workman,J.L. (1998) Perturbation of nucleosome core structure by the SWI/SNF complex persists after its detachement, enhancing subsequent transcription factor binding. *Proc. Natl Acad. Sci. USA*, **95**, 4947–4952.
20. Lorch,Y., Zhang,M. and Kornberg,R.D. (1999) Histone octamer transfer by a chromatin-remodeling complex. *Cell*, **96**, 389–392.
21. Tsanev,R., Russev,G., Pashev,I. and Zlatanova,J. (1993) *Replication and Transcription of Chromatin*, CRC Press, Boca Raton, FI.
22. Boulard,M., Bouvet,P., Kundu,T.K. and Dimitrov,S. (2007) Histone variant nucleosomes: structure, function and implication in disease. *Subcell. Biochem.*, **41**, 71–89.
23. Govin,J., Escoffier,E., Rousseaux,S., Kuhn,L., Ferro,M., Thevenon,J., Catena,R., Davidson,I., Garin,J., Khochbin,S. *et al.* (2007) Pericentric heterochromatin reprogramming by new histone variants during mouse spermiogenesis. *J. Cell Biol.*, **176**, 283–294.
24. Angelov,D., Molla,A., Perche,P.-Y., Hans,F., Côté,J., Khochbin,C., Bouvet,P. and Dimitrov,S. (2003) The histone variant macroH2A interferes with transcription factor binding and SWI/SNF nucleosome remodeling. *Mol. Cell*, **11**, 1033–1041.
25. Doyen,C.M., Montel,F., Gautier,T., Menoni,H., Claudet,C., Delacour-Larose,M., Angelov,D., Hamiche,A., Bednar,J., Faivre-Moskalenko,C. *et al.* (2006) Dissection of the unusual structural and functional properties of the variant H2A.Bbd nucleosome. *EMBO J.*, **25**, 4234–4244.
26. Zhou,J., Fan,J.Y., Rangasamy,D. and Tremethick,D.J. (2007) The nucleosome surface regulates chromatin compaction and couples it with transcriptional repression. *Nat. Struct. Mol. Biol.*, **14**, 1070–1076.
27. Jin,C. and Felsenfeld,G. (2007) Nucleosome stability mediated by histone variants H3.3 and H2A.Z. *Genes Dev.*, **21**, 1519–1529.
28. Angelov,D., Verdel,A., An,W., Bondarenko,V., Hans,F., Doyen,C.M., Studitsky,V.M., Hamiche,A., Roeder,R.G., Bouvet,P. *et al.* (2004) SWI/SNF remodeling and p300-dependent transcription of histone variant H2ABbd nucleosomal arrays. *EMBO J.*, **23**, 3815–3824.
29. Bao,Y., Konesky,K., Park,Y.J., Rosu,S., Dyer,P.N., Rangasamy,D., Tremethick,D.J., Laybourn,P.J. and Luger,K. (2004) Nucleosomes containing the histone variant H2A.Bbd organize only 118 base pairs of DNA. *EMBO J.*, **23**, 3314–3324.
30. Gautier,T., Abbott,D.W., Molla,A., Verdel,A., Ausio,J. and Dimitrov,S. (2004) Histone variant H2ABbd confers lower stability to the nucleosome. *EMBO Rep.*, **5**, 715–720.
31. Wu,C. and Travers,A. (2004) A 'one-pot' assay for the accessibility of DNA in a nucleosome core particle. *Nucleic Acids Res.*, **32**, e122.
32. Luger,K., Rechsteiner,T.J. and Richmond,T.J. (1999) Expression and purification of recombinant histones and nucleosome reconstitution. *Methods Mol. Biol.*, **119**, 1–16.
33. Li,B., Howe,L., Anderson,S., Yates,J.R. 3rd and Workman,J.L. (2003) The Set2 histone methyltransferase functions through the phosphorylated carboxyl-terminal domain of RNA polymerase II. *J. Biol. Chem.*, **278**, 8897–8903.
34. Angelov,D., Bondarenko,V.A., Almagro,S., Menoni,H., Mongelard,F., Hans,F., Mietton,F., Studitsky,V.M., Hamiche,A., Dimitrov,S. *et al.* (2006) Nucleolin is a histone chaperone with FACT-like activity and assists remodeling of nucleosomes. *EMBO J.*, **25**, 1669–1679.
35. Doyen,C.M., An,W., Angelov,D., Bondarenko,V., Mietton,F., Studitsky,V.M., Hamiche,A., Roeder,R.G., Bouvet,P. and Dimitrov,S. (2006) Mechanism of polymerase II transcription repression by the histone variant macroH2A. *Mol. Cell Biol.*, **26**, 1156–1164.
36. Hayes,J.J. and Lee,K.M. (1997) In vitro reconstitution and analysis of mononucleosomes containing defined DNAs and proteins. *Methods*, **12**, 2–9.
37. Montel,F., Fontaine,E., St-Jean,P., Castelnovo,M. and Faivre-Moskalenko,C. (2007) Atomic force microscopy imaging of SWI/SNF action: mapping the nucleosome remodeling and sliding. *Biophys. J.*, **93**, 566–578.
38. Dubochet,J., Adrian,M., Chang,J.J., Homo,J.C., Lepault,J., McDowall,A.W. and Schultz,P. (1988) Cryo-electron microscopy of vitrified specimens. *Q Rev. Biophys.*, **21**, 129–228.
39. Eirin-Lopez,J.M., Ishibashi,T. and Ausio,J. (2008) H2A.Bbd: a quickly evolving hypervariable mammalian histone that destabilizes nucleosomes in an acetylation-independent way. *FASEB J.*, **22**, 316–326.
40. Gonzalez-Romero,R., Mendez,J., Ausio,J. and Eirin-Lopez,J.M. (2008) Quickly evolving histones, nucleosome stability and chromatin folding: all about histone H2A.Bbd. *Gene*, **413**, 1–7.
41. Claudet,C., Angelov,D., Bouvet,P., Dimitrov,S. and Bednar,J. (2005) Histone octamer instability under single molecule experiment conditions. *J. Biol. Chem.*, **280**, 19958–19965.
42. Bednar,J., Horowitz,R.A., Dubochet,J. and Woodcock,C.L. (1995) Chromatin conformation and salt-induced compaction: three-dimensional structural information from cryoelectron microscopy. *J. Cell Biol.*, **131**, 1365–1376.
43. Chaban,Y., Ezeokonkwo,C., Chung,W.H., Zhang,F., Kornberg,R.D., Maier-Davis,B., Lorch,Y. and Asturias,F.J. (2008) Structure of a RSC-nucleosome complex and insights into chromatin remodeling. *Nat. Struct. Mol. Biol.*, **15**, 1272–1277.
44. Leschziner,A.E., Saha,A., Wittmeyer,J., Zhang,Y., Bustamante,C., Cairns,B.R. and Nogales,E. (2007) Conformational flexibility in the chromatin remodeler RSC observed by electron microscopy and the orthogonal tilt reconstruction method. *Proc. Natl Acad. Sci. USA*, **104**, 4913–4918.
45. Smith,C.L., Horowitz-Scherer,R., Flanagan,J.F., Woodcock,C.L. and Peterson,C.L. (2003) Structural analysis of the yeast SWI/SNF chromatin remodeling complex. *Nat. Struct. Biol.*, **10**, 141–145.